DOE/ER/60764--T1

DE93 011620

FINAL REPORT

CELL SPECIFIC RADIATION DOSIMETRY IN SKELETON FROM LIFE-SPAN CARCINOGENESIS STUDIES

Webster S.S. Jee, Ph.D.

DOE CONTRACT NO.: DEFG0289ER60764

DOE FUNDING OFFICE: USDOE/COO

GRANT PERIOD: 1/23/89 TO 1/22/92
1/23/92 TO 1/22/93 (Extension with no funding).

DOE FINAL SCIENTIFIC AND TECHNICAL REPORT: April 5, 1993

Address Correspondence to:

Webster S.S. Jee, Ph.D.
Radiobiology Division
Building 586
University of Utah
Salt Lake City, UT 84112
Telephone: (801) 581-6366
FAX: (801) 581-7008

DOE-6003 FINAL REPORT

THE RESEARCH GRANT

Cell Specific Radiation Dosimetry in the Skeleton from Lifespan Carcinogenesis Studies.

The osteogenic sarcoma is the dominant life-threatening pathology in lifespan studies of beagles exposed to alpha-emitting bone-seeking radionuclides. It was deduced from these studies that certain skeletal sites are more prone to develop tumors. This project will determine the bone cells at risk and their cell-specific radiation dose. The cell-specific radiation dose values will be used to relate to loss and high Ra-226 and Pu-239 induced osteogenic sarcoma sites, to test different dose response hypothesis and predict the extent of effects in humans.

Gaps in Knowledge and Specific Aims. We are still missing knowledge in the following critical areas, which prevents us from completing cell-specific dosimetry:

1. target cell morphometry, origin and fate;
2. cell residence time and proliferation;
3. 239-Pu microdistribution ;
4. 226-Ra microdistribution.

The aim of our studies is to fill the gaps and develop software which calculates cell-specific dose when given appropriate input variables.

The Specific Aims section summarizes the tasks which we propose. Briefly, these include:

1. doing experiments on a rat cortical bone remodeling model system to collect information on the cell kinetics of bone-lining cells and preosteoblast cells;
2. characterizing bone-lining cell and preosteoblast cell morphometry of sites during the bone remodeling sequence (resting, activation, resorption and formation);
3. quantitating bone turnover to determine cell residence time at bone surfaces in different propensities to develop osteosarcoma after 239-Pu or 226-Ra injection in young adult beagles;
4. quantitating the microdistribution of 239-Pu and 226-Ra on bone surface, mineral and marrow in previously serially sacrificed beagles;
5. determining the fate of bone-lining cells during bone remodeling;
6. developing model of bone cell specific dosimettry of 239-Pu and 226-Ra, and
6. developing software to make bone cell-specific radiation dose calculations.

MILESTONES. (This was to be a 6-year program).

1. Year 1:

   1) Refine the rat cortical bone remodeling model system (Specific Aim 1).

   2) Collect information on bone cells at risk in a rat cortical bone remodeling system. The data needed were the characteristics of the bone cells resting within the range of bone-seeking alpha emitters deposited on bone surface and the cell kinetics of bone-lining cells and preosteoblast cells (Specific Aims 1 and 2).

   3) Begin development of a semi-automated system to analyze neutron-induced autoradiographs from 239-Pu contaminated bone sections (Specific Aim 4).

   4) quantitate microdistribution of 226-Ra in bone tissue (Specific Aim 4).

2. Year II.

   1) Begin study to label bone-lining cells in rat cortical bone remodeling system.

   2) Begin study of bone cell residence time in 6 cancellous and 6 cortical bone sites in the Beagle and St. Bernard dog (Specific Aim 3).

   3) Continue quantitation of 226-Ra in bone tissue (Specific Aim 4).

   4. Continue quantitation of 239-Pu in bone tissue (Specific Aim 4).

3. Year III.

   1) Continue study of labeled bone-lining cells in rat cortical bone remodeling system. It will determine the origin of the bone-lining cells, morphometry

   2) Continue measuring microdistribution of 226-Ra in select bones.

   3) Continue measuring microdistribution of 239-Pu in select bones.

4. Year IV.

   1) Begin study of the fate of bone-lining cells during bone remodeling (label bone-lining cells and activate it with lactation and low calcium). (Specific Aim 5).

   2) Continue microdistribution of Ra-226-Ra and 239-Pu studies.

5. Year V.

   1) Complete fate of bone-lining cells study (Specific Aim 5).

   2) Continue microdistribution of 226-Ra and 239-Pu.

   3) Begin development of bone cells and specific dosimetry model of 239-Pu and 226-Ra in the adult skeleton (Specific Aim 6).

6. Year VI.

   1) Complete bone cell specific dosimetry model of 239-Pu and 226-Ra n the adult skeleton.

   2) Develop software to calculate bone-specific dosimetry in sites with different propensities to develop osteosarcomas after 226-Ra and 239-Pu injection in young adult Beagles (Specific Aim 7).

FUNDING.

A 3-year grant was awarded (1989 to 1992) and an additional extension year was requested to complete some studies without funding. During the extension, we had hoped to catch up with our writing. A continuation grant was not submitted because there was never sufficient funds in the budget to pay trained and recent co-investigators. Also, it was morally incorrect to train post-doctoral fellows to do research in an area when there are no jobs for them in the future; thus, funds for the Years IV to VI studies were never requested.

ACCOMPLISHMENTS DURING GRANT PERIOD.

A. Technical Accomplishments:

1) The index of trabecular connectivity (the modal and free end determination) has been automated and added to our analyses of trabecular architecture. We have routinely employed Parfitt's calculated trabecular number, width and separations (Chen et al., 1992; Ke, Li and Jee, 1992).

2) The closure of the distal tibial epiphyses at 3 months makes it a good site to det ermine the response of an adult long bone epiphysis and metaphysis to a given agent, in the absence of local endochondral bone formation. Younger instead of aged rats could be used. The distal tibia contains adequate trabeculation for study. More importantly, we now have part of an adult long bone that is not drifting with growth, allowing one to determine the impact of an agent on cancellous bone remodeling and whether it can activate bone formation without resorption (modeling in the formation mode; Ito et al, in press; Ke et al., in press).

A procedure has been developed to determine quantitatively the local distribution of 239-Pu in bone from neutron-induced autoradiographs (NIARs). The method provides a reliable and statistically valid basis for the evaluation of all essential parameters necessary for local dosimetry. A number of frames, sufficient to provide statistically valid data, are randomly selected from the NIAR and photographed through a microscope. These photographs are projected onto a programmed digitizing table that is connected to a desk top computer. The image of the bone features and the fission tracks are traced manually and converted into their digitized representations. Tracks are assigned separately to bone volume, bone marrow and bone surfaces. Special track patterns such as lines of tracks representing Pu in buried initial surface deposits, diffuse tracks in 'packets' of new bone with a visible track distribution, and clusters of Pu in marrow (stars) are traced as well. All numerical and pictorial information is accessible for further computer processing. An improved procedure to convert fission track densities to local Pu concentrations and to correct for fission tracks originating from

slanted bone surfaces is presented. (Bruenger, Polig and Jee, Radiat. Protection Dosimetry, 35:149-157, 1991).

SCIENTIFIC ACCOMPLISHMENTS.

I. Microdistribution of 239-Pu and 226-Ra in Beagle Dog Bones.

1) A procedure was developed to determine quantitatively the local distribution of 239-Pu in bone from neutron-induced autoradiographs (Bruenger, Polig and Jee, Radiat. Protection Dosimetry, 35:149-157, 1991).

2) We are currently summarizing the data from serially sacrificed Beagle dogs injected with 3.7 K Bq 239-Pu/kg for publication (See enclosed data sheet; Table I).

3) The microdistribution of 226-Ra in the proximal ulna and lumbar vertebral body from bone sections of Beagle dogs receiving a single injection of 355 or 37 K Bq/kg has been published. The intense irradiation in the high level animals led to abnormal formation that was not seen at the lower level (Polig and Jee, Brit. Inst. Radiology Rept.m 21:77-82, 1989).

4) The microdistribution of 226-Ra in the lumbar vertebral body, proximal ulna, and distal femoral metaphysis and epiphysis from bone sections of Beagle dogs injected with 38 K Bq 226-Ra/kg and serially sacrificed at 4 to 2955 days postinjection has been completed. The time-dependent changes in the average 226-Ra concentrations were analyzed by a compartmental model. At 2955 days, the nuclei of bone-lining cells received a maximum dose of 8 Gy in the proximal ulna and a minimum dose of 0.63 Gy in the lumbar vertebra, corresponding to 17 and 1.4 α-particle hits to the cell nuclei (Polig, Jee, Setterberg and Johnson, Radiat. Res. 131:24-34, 1992).

II. Cell-specific Dosimetry Modeling.

1) Radiation dose factors for α–emitters in osteons and some considerations on dose non-uniformity ratios and relative distribution factors. Dose factors for locations within a tissue-filled cylindrical cavity bounded by an infinite medium of bone labeled with an α-emitter are calculated by means of a Monte Carlo procedure. The calculational approach is general and allows us to determine dose factors for specific distances or target volumes defined by concentric cylinders, as well as various source geometries including surface sources, buried surface sources, infinite and bounded volume sources, and also comprises plane (trabecular) surfaces as a limiting case. General expressions for calculating non-uniformity factors and relative distribution factors are derived and implications are discussed in the light of some experimental findings (Polig, Phys. Med. Biol. 34:353-367, 1989)

2) Bone Structural Parameters, Dosimetry, and Relative Radiation Risk in the Beagle Skeleton. From the fractional retention in each part of the skeleton, the initial surface

concentration of 239-Pu after a single injection of 595 Bq/kg body wt (0.016 μCi/kg) on resting surfaces and at sites of bone formation is calculated for various values of the affinity ratios of trabecular/cortical and forming/resting surfaces. These estimated concentrations then yield dose rates as well as cumulative and collective doses to bone-lining cells and osteoblasts in the different parts of the skeleton. On the assumption that the relative risk of tumor induction is proportional to the collective dose to either bone-lining cells or osteoblasts, the frequency of tumor occurrence is calculated and compared to observed frequencies. Both hypotheses yield approximate agreement with experimental data for different ratios of trabecular/cortical radiation sensitivity, although the differences between some bones are statistically significant (Polig and Jee, Radiat Res. 120:83-101, 1989).

3. Kinetic Model of the Distribution of 239-Pu in the Beagle Skeleton. A model was presented to analyze the retention of Pu in the major deposition organs of the beagle dog and predict the dynamic behavior of skeletal labels. The kinetic part describing the gross organ distribution was represented by a compartment model. The model may be applied to single bones or the skeleton as a whole. The flow of Pu in the blood can be derived in hum n cases where urinary excretion rates are available. With the blood flow known, the model enables one to stimulate the dynamic behavior of skeletal labels even for very general conditions of human contamination, including inhalation (Polig, Health Phys. 57:449-660, 1989).
4. A Model of Osteon Closure in Cortical Bone. A model of osteon closure is presented that incorporates some physiologic features of cortical bone remodeling, such as matrix synthesizing activity of osteoblasts, their burial as osteocytes, and elimination of cells. There is a general need for models of this type, not only as a test for our understanding of the bone remodeling mechanism, but also as a tool in instances where a quantitative relationship between bone formation processes and cell populations is of practical importance. For instance, for the microdosimetry of bone-seeking radionuclides during the evolution of secondary haversian systems, models of this kind can be extremely helpful or may even represent the sole basis from which calculations are risk estimations are derived (Polig and Jee, Calcif. Tiss. Int., 47:261-269, 1990).
5. Hit Rates and Radiation Doses to Nuclei of Bone Lining Cells from α-Particle-Emitting Radionuclides. Factors relating the local concentration of a bone-seeking α-particle emitter to the mean hit rate have been determined for nuclei of bone-lining cells using a Monte Carlo procedure. The mean nuclear dose per hit, the dose mean per hit, the mean track segment length and its second moment, the percentage of stoppers, and the frequency distribution of the dose have been determined. Some basic features of the hit

statistics for bone-lining cells have been outlined, and the consequences of existing standards of radiation protection with regard to the hit frequency to cell nuclei are discussed (Polig, Jee and Kruglikov 131:133-142, 1991).

III. Cells at Risk: Their Cellular Kinetics and Bone Histomorphometry.

1. A Review of Bone-lining Cells was published (Miller and Jee, In: Bone, Vol. 4: Bone Metabolism and Mineralization, B.K. Hall (ed.), CRC Press, Boca Raton, FL. pp. 1-19, 1992).
2. Bone Cell Kinetics of Endocortical Remodeling-induced by Lactation and Low Calcium Diet in the Rat. Skeletal responses were limited to endocortical surface. During lactation plus low calcium period, massive resorption was observed at day 3 and it occupied the entire endocortical surface at day 7. However, endocortical resorption began to decrease at day 14 and complete suppressed at day 21. Unexpectedly, despite the continuous severe calcium deficiency, 20% of the endosteal surface was forming bone at day 14 and it extended to all previously resorbed surfaces which included both endocortical and all intracortical cavity surfaces at day 21. We had previously assumed that the reversal phase (bone formation) would not begin until rats were placed on a normal-calcium diet. Numerous bone-lining cells at day 7 of the recovery appeared. The data indicated that the maximum cell proliferation occurred at the 7th day of low-calcium diet and lactation for osteoclasts and at the 3rd day of normal-calcium diet recovery for osteoblasts. However, their precursor cells differentiation peaked approximately 4 - 7 days earlier (Figs. 1 and 2; Jee and Ke, in preparation).
3. Origin of Bone-lining Cells. We labeled a whole generation of osteoblasts by multiple labeling and traced the fate of the osteoblasts thereafter by serial sacrifice. Osteoprogenitor cells declined gradually during the recovery period. The density of total osteoprogenitor cells was 78.6 cells per mm endocortical surface at day 0 of recovery, and decreased to 37.7 at day 21 of recovery. Approximately 50% of osteoprogenitor cells were labeled with ^{3}H-Thymidine at day 0 of recovery, and only 1% of them were labeled with ^{3}H-Thymidine at day 21 of recovery.

   Surface density of osteoblasts decreased dramatically between day 0 and day 7 of recovery (from 98.1 cells per mm endocortical surface to 24.8), and then further decreased between days 14 and 21 of recovery (27.1 cells per mm endocortical surface to 7.8). At day 0 of recovery, 37.8% of osteoblasts were labeled with ^{3}H-Thymidine, and this number increased to 77.1% at day 7, and then decreased to 35.2% and 37.5% at days 14 and 21 of recovery.

   No bone-lining cell was found at day 0 of recovery. Surface density of bone-lining cell increased after 7 days of recovery (27.5 cells per mm endocortical surface at day 7, 37.9

at day 14 and 54.4 at day 21). Fifty-five percent of bone-lining cells were labeled with ^{3}H-Thymidine at day 7 of recovery and maintained in 63.6% and 62.4% at days 14 and 21 of recovery (Figs. 3 and 4; Ke and Jee, in preparation).

4. Static and Dynamic Histomorphometry of Select Cortical and Cancellous Bone Sites. Three- and nine-year-old Beagle dogs were studied. The cortical bone sites included the mid-femoral, proximal humeral, distal humeral, mid-humeral, mid-tibial, mid-metatarsal and rib shafts. The cancellous bone sites involved the proximal tibial, proximal humeral and distal femoral metaphyses, caudal and lumbar vertebral bodies, iliac crest and proximal metatarsal epiphysis.

   A. The major differences between cortical and cancellous bone are its percent mass, surface to volume ratio, and bone formation rates (Table I).

   B. In seven cancellous bone sampling sites, we found that most cancellous bone sites are similar in histomorphometry. The exception is that in the epiphyseal cancellous bone sites there are more bone, smaller surface to volume ratio and lower turnover rates (greater than one order of magnitude).

   C. In six cortical bone sampling sites, we found cortical bone morphometry can be quite variable. One extreme is the mid-femoral shaft with plenty of inner and outer circumferential lamellae that is being remodeled. The other extreme is the rib with greater than average surface to volume ratio, more inner circumferential lamellae and high turnover rate (at least a factor of six greater than other cortical bone sites).

TABLE I. DIFFERENCES BETWEEN CORTICAL AND CANCELLOUS BONES (BEAGLE)

Parameters	Units	Cortical	Cancellous
Mass	%	98	22
Surface/Volume	cm/cm^2	55	180
Mineral Appositional Rate	μm/d	0.77	0.66
Bone Formation Rate	%/yr	43	1.46

(Mori, S., Ke, S.J., Jee, S.S., in preparation).

5. Fate of Labeled Bone-lining Cells After Stimulation of Bone Formation by Prostaglandin E_2 and Parathyroid Hormone. In our previous study entitled "Peak Cell Proliferation during Bone Remodeling", we found that the maximum cell proliferation occurs at the 7th day of low-calcium diet lactation for osteoclasts and at the 3rd day of normal-calcium diet recovery for osteoblasts. Their precursor cells differentiation peaks approximately 4 - 7 days earlier. In a follow-up study, we used multiple ^{3}H-Thymidine labels to label the whole generation of osteoblasts, and we found that the ^{3}H-Thymidine

labeled bone-lining cells were observed after 7 days from the last injection. The current experiment will follow the fate of bone-lining cells when prostaglandin E_2 and parathyroid hormones are employed to accelerate recovery of bone mass from lactation/low calcium diet-induced osteopenia.

Sixty 3-month-old Sprague-Dawley rats and twenty five 3-month-old male rats were used in this study. The female rats were fed low calcium diet during lactation period (21 days) and normal calcium diet during the recovery period (21 days) and normal calcium diet during the recovery period. Multiple injections of ^3H TdR will be given at 5-hour intervals for 48 hours at day 17 to day 18 of the lactation period. Six rats will be sacrificed 1 hour after the last injection. ON day 3 of recovery, a single fluorescent label will be given to the rest of the rats, and one group will be sacrificed. The rest of the rats will be divided into two groups (total 8 subgroups) using prostaglandin E_2 and parathyroid hormone to stimulate the labeled bone-lining cells. Six rats will be double-fluorescent labeled and sacrificed at days 42, 49, 56, 70 and 84 of recovery as listed below:

Diet--Low-calcium from L_1 to L_{21}, normal-calcium diet from R_1 to R^{21}.

Table II. FATE OF BONE-LINING CELLS.

Days	L_{17-18}	RXO_3	R_{42}	R_{49}	R_{56}	R_{70}	R_{84}
	I	X					
	I						X
	I						X
	I						X
	I						X
	I						X
	I						X
	I						X
	I						X
	I						X
	I						X

L = Lactation + low-calcium diet; R = Recovery + normal calcium diet; days from start; X = Kill 6 rats; I = Eight s.c. injections of ^3H Tdr (0.75 μCI/g) at 6 hour intervals; ---- = 6 mg/kg/d of PGE_2 treatment period; **** = 6 μg/kg/d of PTH treatment period.

Schedule for ^3H TdR labeling: (1) Injections of 3H TdR (0.75 μCi/g) at 6 hour intervals for 48 hours will be given as above. Fluorescent label: Recovery day 3 and double-label before sacrifice.

Status of Studies. These animals were treated and sacrificed during the 03 year. Some of the sections and autoradiographs were processed in the 04 year, the extension year without funding. We will try to find time without funding because this is an important study for bone biology and bone radiation biology.

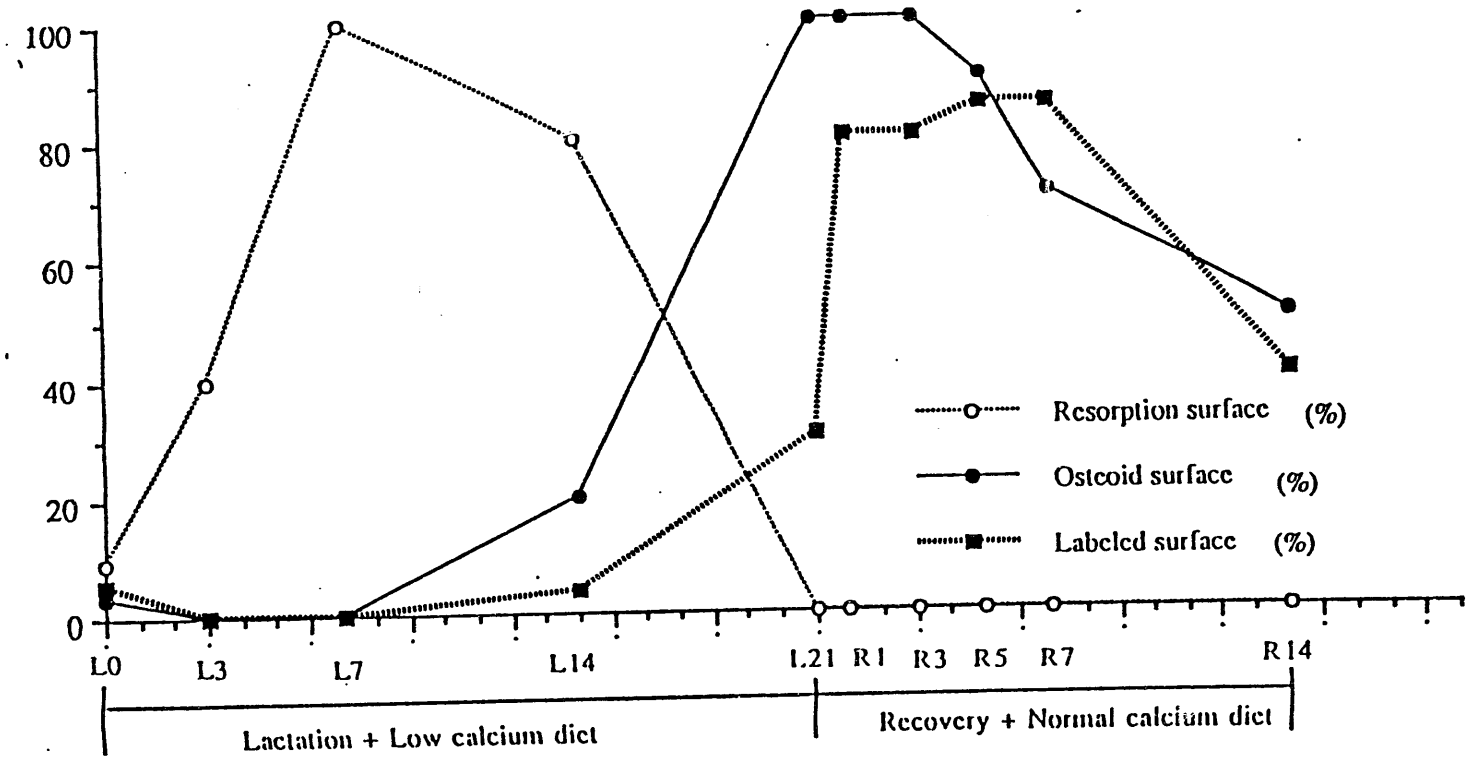

FIG. 1. Distribution of bone surfaces during lactation plus low calcium diet and recovery and normal calcium diet. L0, 3, 7, 14 and 21. 0, 3, 7, 14 and 21 days of lactation; R1, 3, 5, 7 and 14 - 1, 3, 5, 7 and 14 of recovery on normal calcium diet.

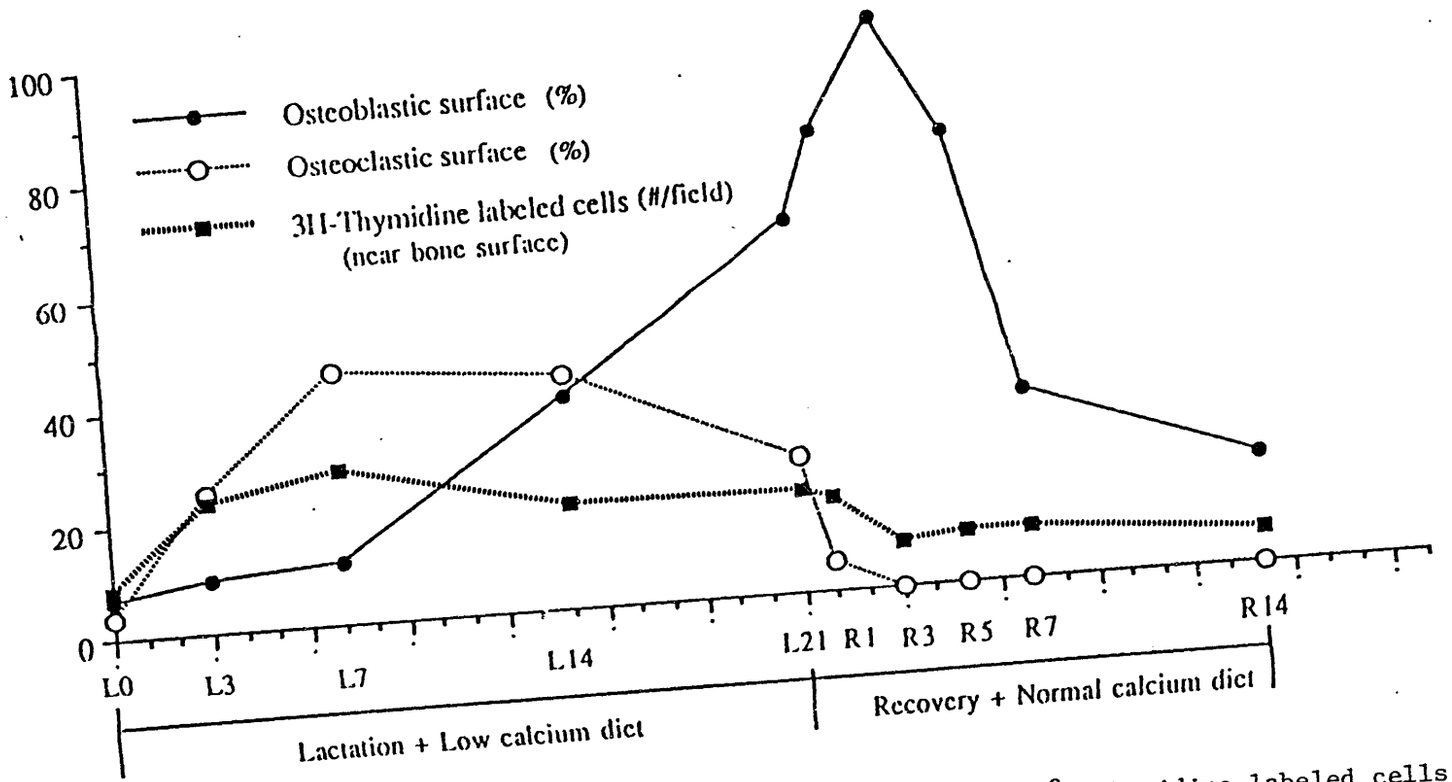

FIG. 2. Distribution of osteoblast and osteoclast surfaces and ^{3}H-thymidine labeled cells near bone surfaces during lactation plus low calcium diet and recovery and normal calcium diet.

PUBLICATIONS:*

1. Bruenger, F.W., Polig, E., Jee, W.S.S. Local distribution of 239-Pu using digitised images of neutron induced autoradiographs. Radiat. Protection Dosimetry, 35; No. 3, 149-157, 1991.
2. Chen, M.M., Jee, W.S.S., Ke, H.Z., Lin, B.Y., Li, Q.,N., Li, X.J. Adaptation of cancellous bone to aging and immobilization in growing rats.
3. Polig, E. Sample page of NIAR Grand Summary, 9/17/90.
4. Ke, H.Z., Li, M., Jee, W.S.S. Prostaglandin E_2 prevents ovariectomy-induced cancellous bone loss in rats. Bone and Mineral 19:45-62, 1992.
5. Lloyd, R.D., Bruenger, F.W., Miller, S.C., Angus, W., Taylor, G.N., Jee, W.S.S., Polig, E. Distribution of radium-induced bone cancers in beagles and comparison with humans. Health Phys. 60:#3:435-438, 1991.
6. Miller, S.C., Jee, W.S.S. Bone lining cells. In: Bone Metabolism and Mineralization, Hall, B.K. (ed). CRC Press, Boca Raton, FL, pp. 1-19.
7. Polig, E. Radiation dose factors for α-emitters in osteons and some considerations on dose non-uniformity ratios and relative distribution factors. Phys. Med. Biol.34: #3; 353-367, 1989.
8. Polig, E. Kinetic model of the distribution of 239-Pu in the beagle skeleton. Health Phys. 57: #3:49-460, 1989.
9. Polig, E, Jee, W.S.S. Bone structural parameters, dosimetry, and relative radiation risk in the beagle skeleton. Radiat. Res. 120:83-101, 1989.
10. Polig, E., Jee, W.S.S. Radium 226 in animals. BIR Report, pp. 77-81, 1989.
11. Polig, E., Jee, W.S.S. A model of osteon closure in cortical bone. Calcif. Tiss. Int. 47:261-269, 1990.
12. Polig E, Jee, W.S.S., Kruglikov, I.L. Hit rates and radiation doses to nuclei of bone lining cells from α-particle-emitting radionuclides. Radiat. Res. 131:133-142, 1992.
13. Polig E, Jee, W.S.S., Setterberg, R.B., Johnson F. Local distribution and dosimetry of 226-Ra in the trabecular skeleton of the beagle. Radiat. Res. 131-24-34, 1992.
14. Woodard, J.C., Jee, W.S.S. Skeleton System. In: Handbook of Toxicologic Pathology, Academic Press, Inc., pp. 489-537, 1991.

*I will try to complete the manuscript in preparation in the near future. It will be difficult because one co-investigator has returned to Japan to his clinical department and two other co-investigators have departed for lucrative positions in industry.

Reprints removed

END

DATE
FILMED
5/13/93